2023 European Conference on Computing in Construction
40th International CIB W78 Conference
Heraklion, Crete, Greece
July 10-12, 2023

DIAGNOSIS OF SIMULTANEOUS SENSOR FAULTS IN STRUCTURAL HEALTH MONITORING SYSTEMS

Thamer Al-Zuriqat, Carlos Chillón Geck, Kosmas Dragos, and Kay Smarsly
Hamburg University of Technology, Hamburg, Germany

Abstract

Current fault diagnosis concepts in structural health monitoring (SHM) are limited by the sole consideration of single sensor faults, which does not fully capture the complexity of real-world faults in SHM systems. This work presents an adaptive fault diagnosis approach for SHM systems that addresses multiple sensor faults occurring simultaneously. The proposed approach, based on analytical redundancy, includes fault detection, isolation, and accommodation, and has been validated using real-world sensor data recorded from a railway bridge. The results show the high accuracy, reliability, and performance of the proposed approach regarding multiple sensor faults that occur simultaneously in real-world SHM systems.

Introduction

In recent years, structural maintenance of civil infrastructure has increasingly relied on structural health monitoring (SHM), which builds upon the acquisition and analysis of monitoring data using sensors (Law et al., 2014). Motivated by safety and cost efficiency, SHM systems reduce maintenance costs and provide continuous information on the structural condition (Liu & Nayak, 2012). Assisting maintenance activities by filling the gaps of periodic visual inspections, SHM systems can help prevent complete failures of civil infrastructure. However, reliability, performance, and synchronization of sensors in SHM systems depend on the accurate operation of the sensing equipment (Dragos et al., 2018).

Caused by hardware or software malfunctions, power outage, environmental impacts, or signal interferences (Li et al., 2019), sensor faults may compromise the reliability and performance of a monitoring system. The most common sensor faults include bias, complete failure, complete failure with noise, gain, drift, and outliers (Zhang et al., 2018). Based on either physical or analytical redundancy, sensor fault diagnosis (FD) approaches for monitoring systems, including SHM systems, have been proposed to detect, isolate, identify, and accommodate sensor faults (Patton, 1990).

To mitigate maintenance, power consumption, and high costs required by physical redundancy, analytical redundancy approaches have been proposed. Analytical redundancy uses mathematical models to describe a system and takes advantage of redundant information inherent in the sensor data to perform FD (Smarsly & Law, 2014). In general, fault detection in analytical redundancy approaches relies on residuals between sensor data and "virtual outputs" estimated by the mathematical models. Then, a threshold logic or a hypothesis testing is used to detect faults (Esserman & Bale, 1997).

Motivated by the complex and – sometimes – nonlinear relationships within the sensor data, artificial intelligence (AI), a special class of mathematical models, is frequently used for sensor FD. In this context, neural networks have extensively been used in FD for SHM. Multilayer neural networks have been used to detect faults in mechanical components of wind turbines (Zaher et al., 2009). Artificial neural network (ANN) models have been embedded into wireless sensor nodes for autonomously detecting and isolating sensor faults in a decentralized manner (Smarsly & Law, 2014). Furthermore, the approach proposed in Smarsly & Law (2014) has been extended from the time-domain to the frequency-domain for FD (Dragos & Smarsly, 2016). A combination of ANN models and convolutional neural network models also has been introduced for full FD, using ANN models for sensor fault detection, isolation, and accommodation and convolutional neural networks for fault identification (Fritz et al., 2022). However, analytical redundancy approaches for SHM have been limited to the diagnosis of sensor faults occurring in individual sensors at different times, thus hampering the application to real-world SHM systems where faults in multiple sensors may occur at the same time ("simultaneous sensor faults").

SHM systems for civil infrastructure have traditionally focused on individual sensor faults without considering the occurrence of simultaneous faults in multiple sensors. Nonetheless, simultaneous faults have been a matter of interest in other disciplines. In the chemical industry, for example, simultaneous sensor and actuator faults have been addressed using a descriptor fuzzy sliding-model observer (Liu et al., 2013). In the domain of aviation and flight-control systems, signals in a finite-frequency domain and simultaneous actuator faults of quadrotor unmanned aerial vehicles have been detected using adaptive fuzzy state estimators and integral terminal sliding-model control (Malayali & Fakir, 2020). Moreover, an analytical redundancy approach has been proposed to detect and isolate faults of multiple sensors in heating, ventilation, and air conditioning (HVAC) systems (Repay et al., 2013), for which robustness and scalability also have been investigated (Papadopoulos et al., 2020).

In summary, despite the large body of research conducted on FD in SHM of civil infrastructure, most approaches address sensor faults occurring in individual sensors (Samee et al., 2011), where only one sensor is faulty (Zhang et al., 2018), and do not consider sensor faults occurring in multiple sensors simultaneously. To extend

FD in SHM towards simultaneous sensor faults in multiple sensors, this paper presents an adaptive FD approach based on analytical redundancy (AFDAR). The AFDAR approach builds upon previous work, in which artificial neural networks and signal processing have been proposed for FD in SHM systems (Smarsly & Law, 2014; Fritz et al., 2022; Al-Zuriqat et al., 2023). Therein, the sensor data of individual sensors has been estimated using artificial neural networks, to which correlated sensor data from other – typically neighboring – sensors have been used as input data, addressing single-fault occurrence under the premise that the input data to each ANN is non-faulty. Nevertheless, when several sensors in real-world SHM systems encounter faults simultaneously, the input data for ANN models will include data from the faulty sensors, resulting in contaminated predictions. By contrast, the AFDAR approach proposed in this study combines ANN models with moving averages of individual sensor data to detect, isolate, and accommodate sensor faults in multiple sensors that occur simultaneously. This work does not incorporate fault identification because it is independent of single-fault or multiple-fault occurrences and has been effectively addressed in prior research (Fritz et al., 2022).

This paper is organized as follows: First, the design and implementation of the AFDAR approach are introduced. Then, the validation of the AFDAR approach is described and the results are discussed. Finally, the work presented in this paper is summarized, and an outlook on future work and improvements of the AFDAR approach is proposed.

Design and implementation of the AFDAR approach

In this section, the design and implementation of the AFDAR approach are introduced, comprising four steps, (i) initialization, (ii) fault detection, (iii) fault isolation, and (iv) fault accommodation. A flowchart depicting the workflow of the AFDAR approach is shown in Figure 1. The four steps of the AFDAR approach are briefly discussed in what follows.

Initialization

1. The initialization step starts with exploring correlations inherent in the sensor data to find a set of correlated sensors. Data recorded by sensors in the SHM system undergo a correlation analysis to identify correlated sensors. The result of the correlation analysis determines the number of correlated sensors k. Then, data recorded by correlated sensors $f_{1\to k}(t)$ is "cleaned", i.e. if sensor data from an individual sensor is missing at a specific time window, the same time window is neglected in all correlated sensors.
2. Data from the set of correlated sensors is normalized to have a common scale in the data values during the training process. A minimum-maximum normalization is used for the data recorded by correlated sensors $f_{1\to k}(t)$.

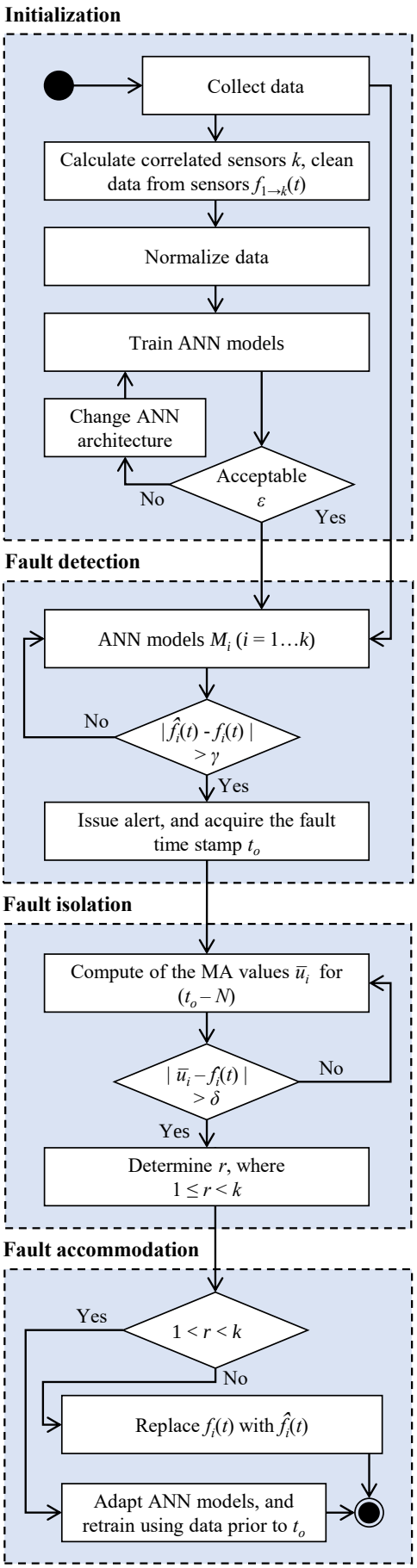

Figure 1: Flowchart of the AFDAR approach.

The formula of the minimum-maximum normalization is depicted in Equation 1, in which x denotes an arbitrary measurement in the sensor data, x_{min} and x_{max} are the minimum and maximum measurements in the sensor data, respectively, and $x_{normalized}$ is the normalized value. The same normalization parameters are applied to newly recorded sensor data fed to the ANN models after training.

$$x_{normalized} = \frac{x - x_{\min}}{x_{\max} - x_{\min}} \quad (1)$$

3. Normalized data is used to train ANN models, with each ANN model "learning" from existing relationships between known input data and known output data. As a result, one ANN model M_i for each correlated sensor i ($i = 1 \ldots k$) is designed and trained using sensor data from the SHM system. During the training of M_i, sensor data from the correlated sensors (1, 2, …, i–1, i+1, …k) is used as input data, and sensor data $f_i(t)$ from sensor i is used as output data. As a result of the training, model M_i estimates virtual outputs of sensor i, denoted by $\hat{f}_i(t)$. The training phase of each ANN model involves selecting the ANN architecture, in terms of the number of hidden layers and the number of neurons per hidden layer. An acceptable ANN architecture is based on the prediction accuracy of the model M_i, lying below the fault detection threshold γ, determined by the root mean squared error (RMSE) value ε between the virtual outputs $\hat{f}_i(t)$ and the sensor data $f_i(t)$, as described in Equation 2. Upon completing the training of the ANN models, the models are deployed on a central computer of the SHM system to automatically detect, isolate, and accommodate sensor faults.

$$\varepsilon = \sqrt{\frac{1}{n}\sum_{i=1}^{n}\left[\hat{f}_i(t) - f_i(t)\right]^2} \quad (2)$$

Fault detection

In this step, newly recorded sensor data is fed into all ANN models. In the event of faults occurring in r sensors ($1 < r < k$), the residuals between the actual sensor data and the virtual outputs in models M_n ($n = 2 \ldots r$) are expected to exceed γ, which, on the one hand, issues a fault detection alert only for the r sensors. The time t_o marking the violation of the fault detection threshold γ serves as the fault time stamp. On the other hand, the faulty sensor data $f_n(t)$ is also used as input for the s models M_v ($v = 1 \ldots s$, $r + s = k$) of the unfaulty sensors, which results in contaminating the virtual outputs of the M_v models and in yielding residual values that also exceed γ. Despite the design and training of ANN models dedicated for each correlated sensor, fault isolation requires further analysis of the sensor data on an individual sensor level. However, conducting the analysis on an individual sensor level requires considering the fault time stamp t_o, which represents the knowledge transferred to the next step.

Fault isolation

Following fault detection, the fault time stamp is utilized to specify a time window N, for which the moving average (MA) values $\bar{u}_i$ of p data points u_{ij} ($j = 1 \ldots p$, $p < N$) are computed for sensor i, as described in Equation 3. The time window should have an adequate length N ($t_o - N$) before the fault time stamp, to ensure reliable tracking of the moving average. Gradual or abrupt changes in the $\bar{u}_i$ values are indicative of sensor faults. As a result, discrepancies between MA values $\bar{u}_i$ and the fault isolation threshold δ from time t_o forward indicate the presence of faulty sensor data in sensor i.

$$\bar{u}_i = \frac{1}{p}\sum_{j=1}^{p} u_{ij} \quad (3)$$

Fault accommodation

Once the fault isolation has been completed and the r faulty sensors have been specified, the ANN models adapt to the new conditions of the SHM system as follows:

1. Adapting the ANN models essentially entails removing sensor data of the r correlated sensors that have been diagnosed as faulty from the ANN input layers of all models. Consequently, the architectures of the ANN models are modified, and retraining the ANN models is necessary for producing virtual outputs for the faulty sensors.
2. Retraining is achieved using sensor data prior to time t_o. Upon completing the retraining, the virtual outputs of the M_n ($n = 2 \ldots r$) models are used as substitutes for the faulty sensor data, thus accommodating the sensor faults.

The thresholds γ and δ depend on the type of data recorded by the SHM system and are, therefore, application-specific. The validation of the AFDAR approach, which uses sensor data from a real-world SHM system, is presented in the next section.

Validation of the AFDAR approach

In this section, the validation test of the AFDAR approach is presented. Data from a real-world SHM system installed at a railway bridge is used to validate the proposed approach, ensuring the accuracy, reliability, and performance of real-world SHM systems where simultaneous faults in multiple sensors may occur.

Description of the railway bridge and of the SHM system

The validation test is carried out using data from an SHM system installed on a composite double-track railway bridge located in Germany. The bridge consists of two parallel steel truss girders that support a 45 cm thick reinforced concrete (RC) slab. The bridge comprises 15 spans, each of 58 m in length, except for the edge spans, which are 57 m in length, and has a total length of 868 m. The deck width is 14.1 m, and the distance between the centroids of the steel truss girders is 6.2 m. Figure 2 illustrates the cross-section of an inner span and the location of embedded temperature sensors in the bridge deck.

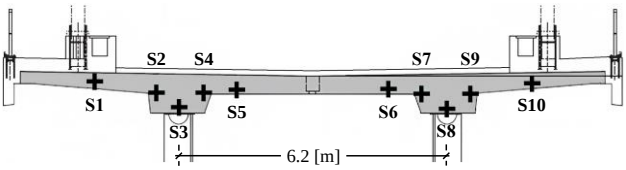

Figure 2: Bridge cross-section and location of temperature sensors.

In this study, sensor data from 10 temperature sensors (S1…S10) embedded in the RC slab is used. The temperature sensors are of type Pt100, measuring at a range from -35 °C to 105 °C with a sensitivity of ± 0.5 °C. Data recorded by the temperature sensors is transferred to a central computer of the monitoring system, where it is stored and processed.

Description of the validation test

The temperature measurements used for validation have been recorded over almost five years with a sampling rate of 1.7 mHz, i.e. one temperature measurement has been recorded every 10 minutes, with a total of 256,000 measurements recorded by each sensor. In the initialization step, correlations between the temperature measurements recorded over a period of two years are investigated via correlation analysis. A strong positive correlation is unveiled by the Pearson correlation coefficient among all 10 temperature sensors belonging to the SHM system; hence, the number of correlated sensors is set to $k = 10$. The lowest correlation coefficient is 0.994 between the sensors S2 and S5. Next, the temperature measurements from the correlated sensors in the SHM system are cleaned and normalized to train the ANN models.

A total of 10 ANN models, equal to the number of correlated sensors ($k = 10$), are trained. Each model predicts the virtual outputs of one sensor, using temperature measurements from the other nine correlated sensors in the SHM system as input data. As a result, each ANN model has nine input neurons and one output neuron; the number of hidden layers and neurons per hidden layer is determined with different ANN architectures. Before training the ANN models for FD, the temperature measurements are split into training and testing sets. An ANN with a 9-32-64-256-256-1 architecture is determined for all ANN models, based on the lowest RMSE values ε, which lie between 0.09 and 0.15, with a total training time of approximately 680 s for each ANN model. The fault detection threshold is set to $\gamma = 0.15$, based upon engineering judgment. Exemplarily, Figure 3 illustrates the architecture of the ANN model M_{10}, which predicts the virtual outputs $\hat{f}_{10}(t)$ for sensor S10 using temperature measurements from correlated sensors $f_{1\to9}(t)$ as input data. With the training of the 10 ANN models, the initialization phase is completed, and the remaining steps of the AFDAR approach, i.e. fault detection, fault isolation, and fault accommodation, are executed separately.

In the validation test, the AFDAR approach is applied to temperature measurements recorded by the SHM system, without prior knowledge of the correct or incorrect operation of the sensors that record the data. The results of the validation test are presented and discussed in the next section.

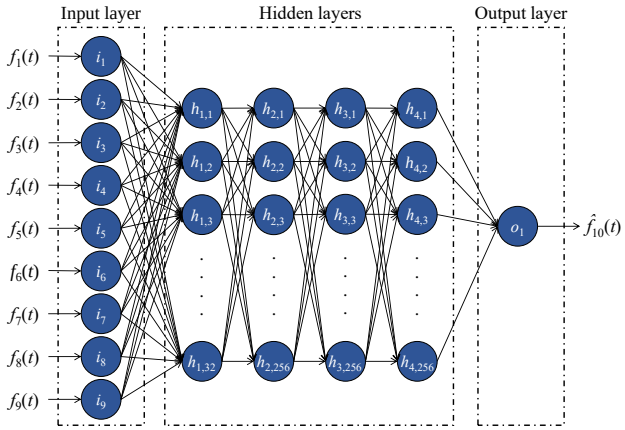

Figure 3: Architecture of the ANN model for sensor S10.

Results and discussion

This section discusses the results of applying the AFDAR approach with temperature measurements newly recorded by the SHM system. The temperature measurements used in the validation test correspond to a period of one year. Specifically, 52,560 temperature measurements are recorded by each sensor. Table 1 introduces the number of faults diagnosed by the AFDAR approach in the newly recorded data.

Table 1: Real-world sensor faults of the SHM system, detected by the AFDA approach

Sensor	Number of faults
S1	0
S2	18
S3	274
S4	0
S5	1
S6	0
S7	0
S8	4,339
S9	0
S10	0
Total	4,632

As presented in Table 1, the AFDAR approach has diagnosed 4,632 faults in the sensor data recorded over one year. To ensure that the proposed AFDAR approach correctly detects real-world sensor faults, and since data is recorded by the same type of sensors (temperature sensors), the data recorded by all temperature sensors is visualized side-by-side. By visualizing and comparing the data, deviations in the faulty sensor data can be observed. Figure 4 shows the data recorded by the correlated sensors in the SHM system, illustratively focusing on faults

detected in sensor S3 and sensor S8. In the figure, the continuous red line represents the data recorded by sensor S3, the continuous green line represents data recorded by sensor S8, and the dotted lines show data recorded by the correlated sensors in the SHM system.

As shown in Figure 4, data recorded by sensor S8 has started deviating from data recorded by the other sensors from December 5. The deviation in the data recorded by sensor S8 may be attributed to a drift. Moreover, no data was recorded by sensor S3 between December 19 and December 20, which may be attributed to a complete failure of the sensor.

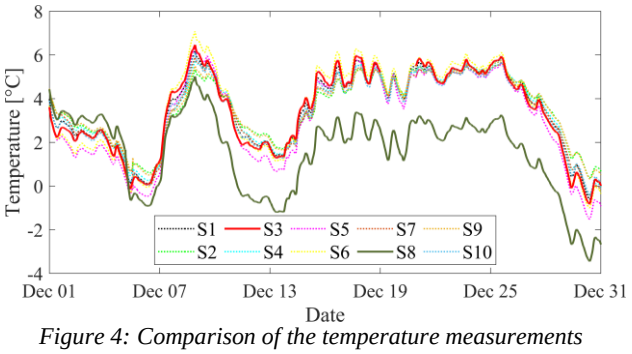

Figure 4: Comparison of the temperature measurements recorded by the SHM system.

Simultaneous faults occurring in sensors S3 and S8 are detected by the AFDAR approach, as the recorded temperature measurements exceed the fault detection threshold, shown in Figure 5. The figure shows data recorded by sensor S3 (top, continuous red line) and by sensor S8 (bottom, continuous green line). The dashed green line shows the virtual outputs of the ANN models, and the dotted black lines represent the fault detection thresholds. It should be noted that a total of 274 simultaneous faults occurred in sensors S3 and S8 between December 19 and December 20; thereupon, the focus is drawn only on simultaneous faults that occurred in the aforementioned period, which fall within the scope of this paper.

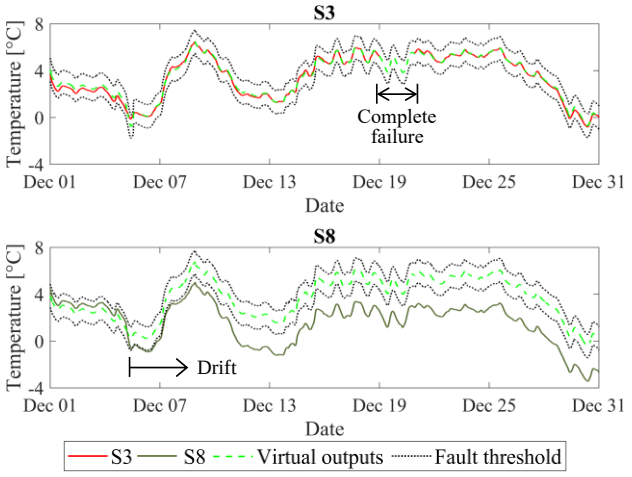

Figure 5: Comparison of temperature measurements and virtual outputs with the fault threshold.

To describe the results of the fault detection, isolation, and accommodation for simultaneous real-world sensor faults, sensors S3 and S8 between December 19 and December 20 are analyzed in more detail. Fault detection is performed when residuals between the temperature measurements from sensors S3 and S8, and the virtual outputs of models M_3 and M_8, exceed the fault detection threshold $\gamma = 0.15$. Then, fault isolation is conducted using the fault time stamp t_o of simultaneous fault occurrence in both sensors S3 and S8, which is determined at t_o = 01:20, on December 19. The fault isolation threshold is set to the accuracy of the temperature sensors $\delta = \pm$ 0.5 °C. Next, observing that residuals between the MA values of sensors S3 and S8 and the respective temperature measurements at t_o exceed the fault isolation threshold δ, the faulty sensors are isolated. Finally, fault accommodation is performed: Since both sensors S3 and S8 are faulty, the models M_3 and M_8 are adapted by modifying the architecture of the ANN models. The ANN architecture is modified by shifting sensors S3 and S8 from the input layer to the output layer, and data prior to t_o is used to train the adapted ANN model $M_{3,8}$. Figure 6 illustrates the architecture of the adapted ANN model $M_{3,8}$, predicting the virtual outputs $\hat{f}_3(t)$ and $\hat{f}_8(t)$ for both sensors S3 and S8.

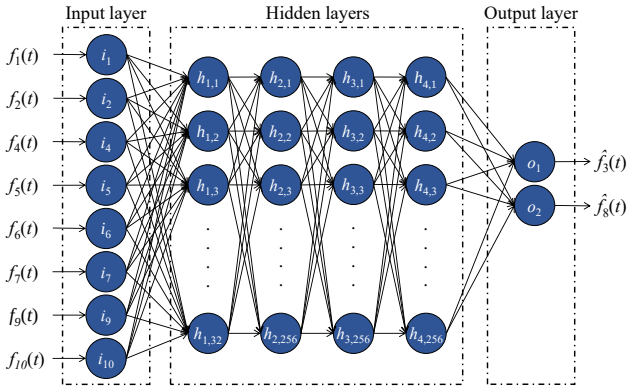

Figure 6: Adapted model $M_{3,8}$ for the sensors S3 and S8.

Summary and conclusions

Sensor faults in monitoring systems, including SHM systems, may affect the quality of monitoring. The SHM community has been showing an increasing interest in adopting sensor FD concepts to ensure the accuracy, reliability, and performance of SHM systems. However, most FD approaches for SHM have been commonly focused on single-fault occurrence without considering simultaneous sensor faults in multiple sensors, which are likely to occur in real-world SHM systems.

This paper has presented an adaptive FD approach based on analytical redundancy (AFDAR), in which simultaneous sensor faults in multiple sensors of SHM systems can be reliably diagnosed. The approach combines ANN models with moving averages of individual sensor data to detect, isolate, and accommodate multiple sensor faults occurring simultaneously. The ANN models are used to predict virtual outputs for each sensor of an SHM system. If residuals between virtual outputs predicted by the ANN models and actual measurements recorded by the sensors exceed a fault detection threshold, a fault detection alert is issued and a

fault time stamp is acquired. To isolate faulty sensors, the moving average of individual sensor data is analyzed and compared with the individual sensor data, recorded around the fault time stamp, with a fault isolation threshold. Finally, faulty data from faulty sensors is replaced with the virtual outputs predicted by the ANN models upon adapting the models by removing faulty sensor data from the input layer during the fault accommodation step. Different from other analytical redundancy approaches reported for fault diagnosis in SHM systems, the AFDAR approach considers multiple sensor faults occurring simultaneously.

To validate the proposed approach, data collected by a real-world SHM system have been used to confirm the accuracy, reliability, and performance of the FD approach to detect, isolate, and accommodate sensor faults. Moreover, the AFDAR approach has been proven capable of adapting to the condition of the SHM system regardless of the number of faulty sensors. In summary, the AFDAR approach can be used to ensure the accuracy of sensors and therefore ensure the reliability and performance of SHM systems.

Future work may focus on extending the AFDAR approach to distinguish between sensor faults and structural damage as well as on improving computational efficiency.

Acknowledgments

The authors gratefully acknowledge the support offered by the German Research Foundation (DFG) under grants SM 281/15-1 and SM 281/20-1, by the German Federal Ministry for Digital and Transport (BMDV) within the mFUND program under grant 19FS2013B, and by the German Federal Ministry of Education and Research (BMBF) under grant 02P20E201. Any opinions, findings, conclusions, or recommendations expressed in this paper are those of the authors and do not necessarily reflect those of DFG, BMDV, or BMBF. The authors gratefully acknowledge the support offered by MKP GmbH in providing sensor data used for validation purposes.

References

Al-Zuriqat, T., Chillón Geck, C., Dragos, K., & Smarsly, K. (2023). Adaptive fault diagnosis for simultaneous sensor faults in structural health monitoring systems. Infrastructures, 8(3), 39.

Dragos, K. & Smarsly K. (2016). Distributed adaptive diagnosis of sensor faults using structural response data. Smart Materials and Structures, 25(10), 105019.

Dragos, K., Theiler, M., Magalhães, F., Moutinho, C. & Smarsly, K. (2018). On-board data synchronization in wireless structural health monitoring systems based on phase locking. Structural Control and Health Monitoring, 25(11), e2248.

Fritz, H., Peralta Abadía, J. J., Legatiuk, D., Steiner, M., Dragos, K. & Smarsly, K. (2022). Fault Diagnosis in Structural Health Monitoring Systems Using Signal Processing and Machine Learning Techniques. Structural Health Monitoring Based on Data Science Techniques, Cury, A., Ribeiro, D., Ubertini, F. & Todd, M. D., Eds. Cham: Springer International Publishing, pp. 143-164.

Isermann, R. & Ballé, P. (1997). Trends in the application of model-based fault detection and diagnosis of technical processes. Control Engineering Practice, 5(5), pp. 709-719.

Law, K. H., Smarsly, K & Wang, Y. (2014). Sensor data management technologies for infrastructure asset management. Sensor Technologies for Civil Infrastructures. Wang, M. L., Lynch, J. P. & Sohn, H. Eds. Woodhead Publishing, pp. 3-32.

Li, L., Liu, G., Zhang, L. & Li, Q. (2019). Sensor fault detection with generalized likelihood ratio and correlation coefficient for bridge SHM. Journal of Sound and Vibration, 442, pp. 445-458.

Liu, M., Cao, X. & Shi, P. (2013). Fuzzy-Model-Based Fault-Tolerant Design for Nonlinear Stochastic Systems Against Simultaneous Sensor and Actuator Faults. IEEE Transactions on Fuzzy Systems, 21(5), pp. 789-799.

Liu, Y. and Nayak, S. (2012). Structural Health Monitoring: State of the Art and Perspectives. The Journal of The Minerals, Metals & Materials Society, 64(7), pp. 789-792.

Mallavalli S. & Fekih, A. (2020). A fault tolerant tracking control for a quadrotor UAV subject to simultaneous actuator faults and exogenous disturbances. International Journal of Control, 93(3), pp. 655-668.

Papadopoulos, P. M., Reppa, V., Polycarpou, M. M. & Panayiotou, C. G. (2020). Scalable distributed sensor fault diagnosis for smart buildings. IEEE/CAA Journal of Automatica Sinica, 7(3), pp. 638-655.

Patton, R. J. (1990). Fault detection and diagnosis in aerospace systems using analytical redundancy. In: IEE Colloquium on Condition Monitoring and Fault Tolerance. London, UK, 11/06/1990.

Reppa, V., Papadopoulos, P., Polycarpou, M. M. & Panayiotou, C. G. (2013). Distributed detection and isolation of sensor faults in HVAC systems. In: The 21st Mediterranean Conference on Control and Automation, Crete, Greece, 06/25/2013.

Samy, I., Postlethwaite, I. & Gu, D.-W. (2011). Survey and application of sensor fault detection and isolation schemes. Control Engineering Practice, 19(7), pp. 658-674.

Smarsly, K. & Law, K. H. (2014). Decentralized fault detection and isolation in wireless structural health monitoring systems using analytical redundancy. Advances in Engineering Software, 73, pp. 1-10.

Zaher, A., McArthur, S. D. J., Infield, D. G. & Patel, Y. (2009). Online wind turbine fault detection through automated SCADA data analysis. Wind Energy, 12(6), pp. 574-593.

Zhang, Z., Mehmood, A., Shu, L., Huo, Z., Zhang, Y. & Mukherjee, M. (2018). A Survey on Fault Diagnosis in Wireless Sensor Networks. IEEE Access, 6, pp. 11349-11364.